Salt-bridge interaction between K26 and E33 is important for maintaining the stability of ALFPm3

Hafeeza Sakor [1], Thassanai Sitthiyotha [2], Surasak Chunsrivirot [2], Phattarunda Jaree [3], Premruethai Supungul [4] and Kunlaya Somboonwiwat [1,*]

[1] Center of Excellence for Molecular Biology and Genomics of Shrimp, Department of Biochemistry, Faculty of Science, Chulalongkorn University, Bangkok 10330, Thailand; 6172113923@student.chula.ac.th
[2] Structural and Computational Biology Research Unit, Department of Biochemistry, Faculty of Science, Chulalongkorn University, Bangkok 10330, Thailand; surasak.ch@chula.ac.th
[3] Center of Applied Shrimp Research and Innovation, Institute of Molecular Biosciences, Mahidol University, Salaya, Nakhon Pathom, Thailand; phattarunda.jar@mahidol.ac.th
[4] National Center for Genetic Engineering and Biotechnology, Thailand Science Park, Phahonyothin Road, Khlong Nueng, Khlong Luang, Pathum Thani 12120, Thailand; premruethai.sup@biotec.or.th
* Correspondence: kunlaya.s@chula.ac.th; Tel.: +66 2 218 5438

Abstract: The shrimp industry has been persistently affected by production loss from outbreak diseases. Nowadays, using antibiotics in animal feed is illegal. Use of antimicrobial peptide is alternative approach to fight against bacterial infection, and anti-lipopolysaccharide factor isoform 3 (ALF*Pm*3) from *Penaeus monodon* is a promising candidate because it exhibits broad-spectrum antimicrobial activities against various microbes. The lipopolysaccharide-binding domain (LPS-BD) mainly contributes to the antimicrobial activity of ALF*Pm*3. Previous studies reported that the recombinant (r)ALF*Pm*3-supplemented diet can be used to control bacterial and viral infection in shrimp and enhance expression of immune-related genes. However, the possibility of applying rALF*Pm*3 for shrimp disease prevention and control is limited by the high production cost. The more effective rALF*Pm*3 is thus needed. This study aims to produce more effective rALF*Pm*3. ALF*Pm*3 derivatives with better predicted binding affinities to LPS than that wild type were designed using computational techniques. ALF*Pm*3$_{E33F}$ was predicted to have the best binding affinity to LPS (ΔG_{bind} = -14.5 kcal/mol). Site-directed mutagenesis was performed to create the rALF*Pm*3$_{E33F}$ mutant. Following expression and purification, we unexpectedly found that the stability of the rALF*Pm*3$_{E33F}$ protein was lower than that of the wild type. Structural analysis shows that the salt-bridge interaction between K26 and E33, a residue flanking LPS-BD, in the wild type is disrupted when E33 was substituted with F33 in ALF*Pm*3$_{E33F}$. Out results indicate that the salt bridge between K26 and E33 is important to maintain the stability of rALF*Pm*3.

Graphical abstract:

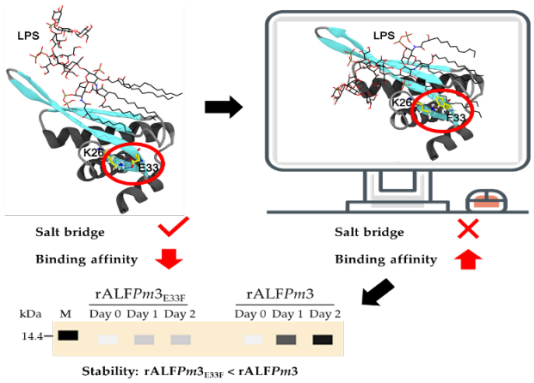

Keywords: Anti-lipopolysaccharide factor isoform 3; Salt-bridge interaction; Protein stability

1. Introduction

Shrimp industry has been persistently affected by production loss from infectious diseases. Pathogenic bacteria, particularly Vibrio species, are a major concern for shrimp larvae and juveniles. For instance, *Vibrio harveyi* and *Vibrio vulnificus* are associated with larvae mortality, whereas *Vibrio alginolyticus*, and *Vibrio parahaemolyticus* cause disease outbreaks in shrimp nurseries. Since 2012, the outbreak of acute hepatopancreatic necrosis disease (AHPND) caused by a highly virulent strain of *V. parahaemolyticus* (VP_{AHPND}) resulted in serious drops in Thai shrimp production [1].

Antibiotics have been used in aquaculture to prevent or treat diseases. The two main effects of antibiotic usage in animal feed are enhancing antibiotic-resistant bacteria and toxicity of antibiotic residues. Nevertheless, antibiotics using in animal feed are illegal [2]. Antimicrobial peptides (AMPs) can eliminate bacteria by nonspecific membrane destruction and metabolic inhibition without inducing bacterial resistance. AMPs are promising candidates for next-generation antibiotics [3].

Anti-lipopolysaccharide factor (ALF) isoform 3 from *Penaeus monodon* (ALF*Pm*3) is a cationic amphipathic molecule containing 98 amino acid residues. The ALF*Pm*3 structure consists of three α-helices packed against a four-stranded β-sheet with two conserved cysteine residues forming a disulfide bond. Positively charged residues clustered within the conserved disulfide loop have been defined as the lipopolysaccharide-binding domain (LPS-BD) [4]. ALF*Pm*3 exhibits broad-spectrum antimicrobial activity against various pathogens. ALF*Pm*3 can bind to LPS of gram-negative bacteria, lipoteichoic acid (LTA) of gram-positive bacteria, β-glucan of fungi, and some enveloped viruses. Previous research revealed recombinant (r)ALF*Pm*3 protein kills the gram-negative bacteria, major bacteria pathogens of shrimp diseases, by bacterial membrane permeabilization. rALF*Pm*3 binds to LPS of the bacteria through ionic interactions and hydrophobic interactions leading to pore formation and cytoplasmic content leaking [5-7]. Furthermore, rALF*Pm*3 was able to reduce the cumulative mortality rate of VP_{AHPND}-infected shrimp. As a potential immunostimulant, researchers reported that a rALF*Pm*3-supplementary diet increases the survival rate of WSSV-infected shrimp by enhancing the transcriptional level of immune-related genes. Taken together, the rALF*Pm*3-supplementary diet can control VP_{AHPND} and WSSV infections in shrimp aquaculture [8]. Unfortunately, using rALF*Pm*3 as a supplementary diet in farming is limited by the high production cost. Therefore, the development of ALF*Pm*3 derivatives with increased effectiveness is necessary.

In this study, computational techniques were used to design ALF*Pm*3 derivatives with better predicted binding affinities to LPS than the wild-type ALF*Pm*3. The designed protein with the best predicted binding affinity was selected for experiments. The more potent ALF*Pm*3 could reduce the production cost, increasing the possibility of applying ALF*Pm*3 for the prevention and disease control in shrimp farming.

2. Materials and Methods

2.1. Computational design of ALFPm3 derivatives

I-TASSER server [9] was employed to construct the structure of ALF*Pm*3 (Accession number: EF523559.1). The ALF*Pm*3 structure was then protonated at the experimental pH (6.5) using the H++ server [10]. The LPS structure was obtained from the crystal structure of the FhuA–LPS complex (PDB entry: 1QFG [11]). Autodock Vina [12] was employed to dock LPS on to LPS-BD of ALF*Pm*3 to determine the reasonable binding conformations of LPS-ALF*Pm*3 complex. The structure of the LPS-ALF*Pm*3 complex was used as a design template to enhance the binding affinity between LPS and ALF*Pm*3. Designed positions were chosen based on the following criteria: (i) they are in the LPS-binding site (within 8

Å of LPS) and (ii) their side chains could potentially form favorable interactions upon mutations with LPS. Each designed position was allowed to be amino acids that could potentially increase favorable interactions with LPS. If it is close to the inner core of LPS, it is allowed to be R, H or K to increase hydrogen bond and electrostatic interactions with the inner core of LPS. However, if it is close to lipid A of LPS, it is allowed to be L, I, M, F, Y or W to increase hydrophobic interaction with lipid A of LPS. The designed structures of ALF*Pm*3 were then constructed and protonated at pH 6.5. Subsequently, LPS was docked on to the designed ALF*Pm*3 to determine the binding energy of the complexes. ALF*Pm*3 with the best predicted binding affinity, where its predicted binding affinity is also better than that of ALF*Pm*3, was selected for experiments.

2.2. Construction of expression vector of designed-ALFPm3 via site-directed mutagenesis technique

The mutagenesis was done according to the instruction manual of QuikChange II Site-Directed Mutagenesis kit (Agilent Technologies, USA). Recombinant pPIC9K containing wild-type ALF*Pm*3 gene [6] was used as a DNA template for mutagenesis. The template was amplified using KOD FX DNA polymerase with site-directed mutagenic primers (Forward primer: 5'CGAAAAAACTGAACTTCTCGGCCACTTCTGCAAGTTCACCGTCAAGCC-3' and Reverse primer: 5'-GGCTTGACGGTGAACTTGCAGAAGTGGCCGAGAAGTTCAGTTTTTTCG-3') to create a designed sequence. Before transformation into XL1-Blue competent cells, the purified PCR product was digested with *Dpn*I restriction endonuclease at 37°C for 3 h. The nucleotide sequence of positive transformants which grew on Luria-Bertani (LB) agar containing ampicillin was sequenced.

2.3. Pichia pastoris (P. pastoris) transformation and recombinant clone selection

According to previously described [6], *P. pastoris* strain KM71 was grown overnight in yeast extract peptone dextrose (YPD) medium at 30°C with vigorous shake. The yeast cells were harvested, washed twice with ice-cold sterile water, and resuspended in 1 M sorbitol. Meanwhile, the designed plasmid was completely linearized overnight by *Sac*I restriction enzyme at 37°C. Five up to ten micrograms of purified-linear plasmid were transformed into the yeast cells by electroporation as described in manufacturer instructions of multi-copy *Pichia* Expression kit (Invitrogen, USA). The cells were spread on minimal dextrose (MD) plates and incubated at 30°C for 3-4 days. Then, the transformants were pooled in sterile water. Positive *P. pastoris* transformants were screened on YPD plates containing 4 mg/ml of G418-sulphate at 30°C until colonies appearance. A single colony was streaked on YPD agar plates containing 4 mg/ml of G418-sulphate several times to purify putative G418-sulphate resistant clones. The purified yeast clone was confirmed by yeast colony PCR using α-factor (Forward primer: 5′-TACTATTGCCAGCATTGCTGC-3′) and 3′AOX (Reverse primer: 5′-AGGATGTCAGA ATGCCATTTGCC-3′) primers. The clones were subsequently confirmed by sequencing before protein expression.

2.4. Expression and purification of rALFPm3 proteins

The rALF*Pm*3 protein was expressed and purified as described previously [6]. In brief, the purified single colonies of designed-ALF*Pm*3 mutant and ALF*Pm*3 producing yeast were separately grown overnight in YPD medium at 30°C with robust shake. The cell cultures were inoculated overnight in Buffered Glycerol-complex (BMGY) medium until an optical density at 600 nanometers (OD_{600}) reached 4-6 and harvested by centrifugation. The cells were transferred into Buffered Methanol-complex (BMMY) medium using 1/5 of the original culture volume to induce the protein expression. 100% methanol was added every 24 h to a final concentration of 0.5% for two consecutive days. The supernatants were collected every 24 h post-induction to check the expression profile of the protein. The crude supernatants were purified using strong cation exchange chromatography with SP Sepharose™ High-Performance resin (GE Healthcare, USA) using binding buffer (20 mM

Tris-HCl pH 7.4 solution with 200 mM NaCl) and elution buffer (20 mM Tris-HCl pH 7.4 solution with 1 M NaCl). The proteins were analyzed on 15% SDS-PAGE and detected by silver staining. Concentration of the crude and purified proteins were measured using Bradford assay [13] and spectrophotometry at 280 nanometers, respectively. The purified proteins were stored at -80°C.

3. Results

3.1. Computational design of ALFPm3 derivatives

Computational techniques were employed to design ALF*Pm*3 derivatives with better predicted binding affinities to LPS than the wild- type ALF*Pm*3, using the binding conformation of LPS binding to ALF*Pm*3 (ΔG_{bind} = -11.8 kcal/mol), as predicted by Autodock Vina, as a template (Figure 1.). In this study, designed positions were selected from the LPS-binding site. If they are close to the inner core of LPS, they are allowed to be R, H, or K. However, if they are close to lipid A of LPS, they are allowed to be L, I, M, F, Y, or W. The docking results of LPS and designed ALF*Pm*3 show that ALF*Pm*3$_{E33F}$ was predicted to have the best binding affinity to LPS (ΔG_{bind} = -14.5 kcal/mol). Therefore, ALF*Pm*3$_{E33F}$ with the best predicted binding affinity to LPS was selected for experiments. Figure 1 shows that the salt-bridge interaction between K26 and E33 in the wild-type ALF*Pm*3 was replaced with the cation-π interaction between K26 and F33 of ALF*Pm*3$_{E33F}$.

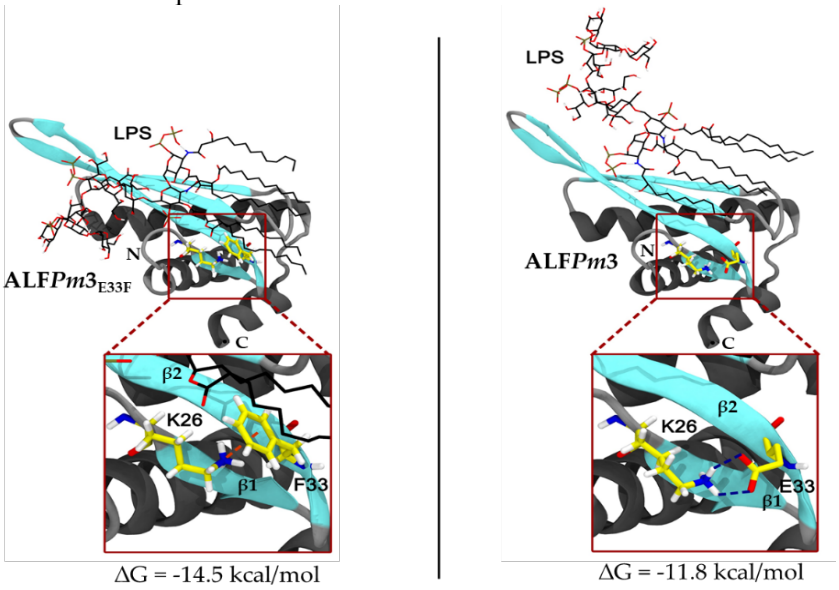

Figure 1. Predicted binding conformations of LPS to ALF*Pm*3$_{E33F}$ (left) and ALF*Pm*3 (right). The secondary structures are represented in ribbon diagram with blue color (β-sheets) and grey color (α-helices). The LPS structure is represented in licorice representation. The interactions between residue 26 and 33 are in the red boxes. Cation–π interaction of K26-F33 (red dash line) and salt-bridge interaction of K26-E33 (blue dash line) are displayed. N and C indicate N-terminus and C-terminus, respectively.

3.2. Molecular cloning

To validate the computational result, site-directed mutagenesis was performed to produce the recombinant mutant clones. The nucleotide sequence of the successful mutated recombinant plasmid possessed an open reading frame (ORF) of 297 bp (data not shown), encoding 98 amino acids (Figure 2.). To obtain a protein expression clone, the mutant cassette was successfully integrated into the genome of *P. pastoris* KM71 strain via electroporation. The purified putative G418-sulphate resistant clones were also confirmed by yeast colony PCR (data not shown) before protein expression in yeast system.

```
ALFPm3E33F    QGWEAVAAAVASKIVGLWRNEKTELLGHECKFTVKPYLKRFQVYYKGRMW   50
ALFPm3        QGWEAVAAAVASKIVGLWRNEKTELLGHECKFTVKPYLKRFQVYYKGRMW   50
ALFPm3E33F    CPGWTAIRGEASTRSQSGVAGKTAKDFVRKAFQKGLISQQEANQWLSS     98
ALFPm3        CPGWTAIRGEASTRSQSGVAGKTAKDFVRKAFQKGLISQQEANQWLSS     98
```

Figure 2. Amino acid alignments of rALF*Pm*3E33F and rALF*Pm*3 proteins. Black highlight indicates mutation site of ALF*Pm*3E33F. LPS-BD is shown as underlined letters.

3.3. rALFPm3 protein production and purification

To compare the efficiency of rALF*Pm*3 mutant and wild-type proteins, ALF*Pm*3E33F and ALF*Pm*3 proteins were expressed in the *P. pastoris* system with methanol induction every 24 h to maintain the induction for two consecutive days. The collected supernatants were determined for their protein expression. The one major proteins with an apparent molecular weight around 11 kDa were detected on the silver-stained SDS-PAGE. However, it is obvious that the expression of rALF*Pm*3E33F protein was extremely lower than the wild type on both days after induction. Moreover, similar intensities of ALFPm3E33F protein were found on the two consecutive days. Whereas the intensity of rALF*Pm*3 protein was significantly increased over time. Corresponding to the total protein concentrations on two days after induction, the crude rALF*Pm*3E33F was 39.9 mg/l and 43.22 mg/ml, respectively. On the contrary, rALF*Pm*3 was 66.24 mg/l and 120.97 mg/ml, respectively (Figure 3.). The crude supernatant of either rALF*Pm*3E33F or rALF*Pm*3 was subjected to purification through cation exchange chromatography (Figure 4.). The concentration of purified rALF*Pm*3E33F was (30.84 mg/ml) 4.4 folds lower than rALF*Pm*3 (134.66 mg/ml). It should be noted that the remaining percent of purified ALF*Pm*3E33F and ALF*Pm*3 proteins at 10 months after purification were 46.77% and 84.76%, respectively (Table 1). This result suggests that rALF*Pm*3E33F has lower production yield and stability as compared with the wild type.

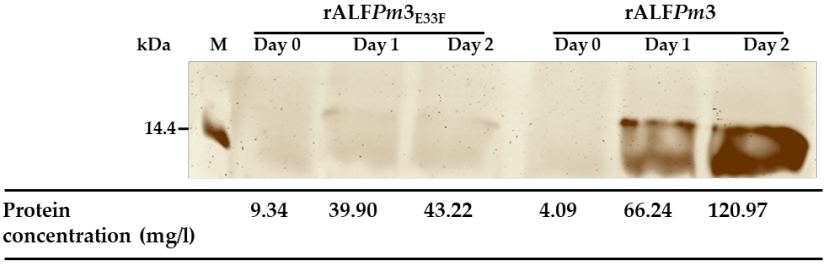

Figure 3. Expression profile of rALF*Pm*3 proteins during methanol induction for two consecutive days in *P. pastoris* system. Crude proteins (50 µl) were analyzed on 15% SDS-PAGE with silver staining detection. The total protein concentration was measured using Bradford assay.

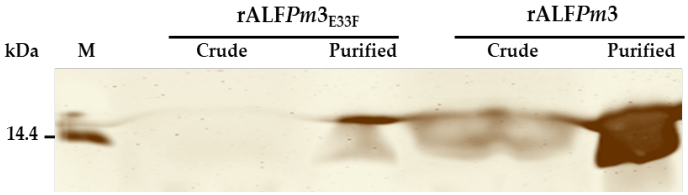

Figure 4. Analysis of the purified rALF*Pm*3 proteins by SDS-PAGE. Crude proteins (50 µl) and purified proteins (20 µl) were analyzed on 15% SDS-PAGE with silver staining detection.

Table 1. Purified protein stability

Protein	Protein concentration (mg/l) (After purification)	Protein concentration (mg/l) (10 months after purification)	Remaining percent (%)
rALF*Pm*3E33F	30.84	14.39	46.77
rALF*Pm*3	134.66	114.10	84.76

4. Discussion

rALF*Pm*3 containing LPS-BD is a highly active antimicrobial peptide that directly kills gram-negative through bacterial membrane permeabilization [5]. LPS, a major cell wall component of gram-negative bacteria, composed of three domains. There are lipid A, inner core, and outer core. Lipid A consists of lipid chains linked to a phosphorylated disaccharide core representing hydrophobic property and polar property of lipid A. The inner core and outer core comprise a large number of hexoses that display hydrophilic properties. However, the inner core also contains phosphate residues showing polar property [11]. rALF*Pm*3 binds to LPS via ionic interactions of seven amino acid residues and hydrophobic interactions of hydrophobic residues located in LPS-BD and the flanking β-strands or flanking α-helices for some hydrophobic residues. The seven amino acids contribute to ionic interaction with LPS such as six positively charged residues (K26, K35, K39, K50, R52, and R62) and one negatively charged residue (E25). These amino acids interact with the polar part of lipid A. The hydrophobic amino acids, i.e., W22, P40, Y41, and Y48, interact with acyl chains of lipid A [7].

In this work, computational techniques were employed to design more potent ALF*Pm*3 proteins with better predicted binding affinities to LPS than the wild type. Results from computational design and docking show that ALF*Pm*3$_{E33F}$ was predicted to have the best binding affinity to LPS (ΔG_{bind} = -14.5 kcal/mol), and its predicted binding affinity is also better than that of ALF*Pm*3 (ΔG_{bind} = -11.8 kcal/mol). Therefore, ALF*Pm*3$_{E33F}$ was selected for experiments. Previous study reported that rALF*Pm*3 protein was gradually increased over time post consecutive methanol induction every 24 h in the *P. pastoris* system [6]. Expression of ALF*Pm*3$_{E33F}$ in *P. pastoris* in comparison with wild type revealed that the production yield of ALF*Pm*3$_{E33F}$ was extremely low. Moreover, remaining percent (10 months after purification) of purified ALF*Pm*3$_{E33F}$ was 2 folds lower than that of ALF*Pm*3. These results suggest that ALF*Pm*3$_{E33F}$ may have much lower stability than the wild-type ALF*Pm*3. The low stability probably caused protein degradation during the expression and purification processes. The low stability of ALF*Pm*3$_{E33F}$ may be caused by the disruption of the salt-bridge interaction between K26 and E33 that holds the β1 and β2 strands together in the wild-type ALF*Pm*3. Although the predicted binding conformation between LPS and ALF*Pm*3$_{E33F}$ contains the cation-π interaction between K26 and F33, this interaction may not be strong enough to hold the β1 and β2 strands together. Furthermore, since E33 is a conserved amino acid of ALF protein, despite the fact that it is not an important amino acid for LPS-recognition of ALF*Pm*3 [7], mutation at this residue may disrupt favorable interactions and cause structural changes of ALF*Pm*3 that affect its stability. Thus, our results suggest that the salt-bridge interaction between K26 and E33 may be important for maintaining the stability of the three-dimensional structure of ALF*Pm*3. Previous studies reported that salt-bridge interactions are crucial for maintaining protein thermostability. A lot of salt-bridge interactions were found in thermophilic proteins [14, 15]. Increasing the number of salt bridges, resulting in the increase of T_m of protein, is one of the most efficient strategies to increase protein thermal stability [16]. Overall, our results provide insight into important interactions of ALF*Pm*3 that are beneficial for designing more potent ALF*Pm*3.

5. Conclusions

In this work, computational techniques were employed to design ALF*Pm*3 derivatives with better predicted binding affinities to LPS than the wild-type ALF*Pm*3. ALF*Pm*3$_{E33F}$ was predicted to bind to LPS with the best binding affinity and was selected for experiments. Experimental results show that the stability of ALF*Pm*3$_{E33F}$ is significantly lower than that of the wild-type ALF*Pm*3. The low stability of ALF*Pm*3$_{E33F}$ is probably caused by the disruption of the salt-bridge interaction between K26 and E33 in the structure of ALF*Pm*3, suggesting that E33 and the salt-bridge interaction between K26 and E33 play important roles in maintain the structural stability of ALF*Pm*3. Our findings provide

insight into interactions that are important for maintaining the stability of ALF*Pm*3, and this knowledge is beneficial for designing more potent ALF*Pm*3 derivatives.

Author Contributions: Conceptualization, K.S. and S.C.; methodology, K.S., P.J., H.S., T. S. and S.C.; validation, H.S., T.S., K.S. and S.C.; investigation, H.S. and T.S.; resources, K.S., P.J. and S.C.; data curation, K.S. and S.C.; writing—original draft preparation, H.S., T.S., K.S. and S.C.; writing—review and editing, H.S., K.S., S.C. and P.S.; visualization, H.S. and T.S.; supervision, K.S. and S.C.; project administration, K.S and S.C.; funding acquisition, S.C. and K.S."

Funding: This research was funded by (Agricultural Research Development Agency (Public Organization) (CRP6405021450). Student fellowship from Thailand Graduate Institute of Science and Technology, "TG-22-09-61-080M" is acknowledged. T.S. and S.C. were partially supported by the Structural and Computational Research Unit, Department of Biochemistry, Faculty of Science, Rachadaphiseksomphot Endowment Fund, Chulalongkorn University, Thailand.

Conflicts of Interest: The funders had no role in the design of the study; in the collection, analyses, or interpretation of data; in the writing of the manuscript, or in the decision to publish the results.

References

1. Thitamadee, S.; Prachumwat, A.; Srisala, J.; Jaroenlak, P.; Salachanb, P.V.; Sritunyalucksana, K.; Flegel, T.W.; Itsathitphaisarn, O.Review of current disease threats for cultivated penaeid shrimp in Asia. *Aquac.* **2016**, *452*, p. 69-87. https://doi.org/10.1016/j.aquaculture.2015.10.028
2. Holmström, K.; Gräslund, S.; Wahlström, A.; Poungshompoo, S.; Bengtsson, B.E.; Kautsky, N. Antibiotic use in shrimp farming and implications for environmental impacts and human health. *Int. J. Food Sci.* **2003**, *38*, p. 255-266. https://doi.org/10.1046/j.1365-2621.2003.00671.x
3. Chen, F.; Tang, Y.; Zheng, H.; Xu, Yang.; Wang, J.; Wang, C. Roles of the Conserved Amino Acid Residues in Reduced Human Defensin 5: Cysteine and Arginine Are Indispensable for Its Antibacterial Action and LPS Neutralization. *ChemMedChem* **2019**, *14*, p. 1457-1465. https://doi.org/10.1002/cmdc.201900282
4. Tassanakajon, A.; Somboonwiwat, K.; Amparyup, P. Sequence diversity and evolution of antimicrobial peptides in invertebrates. *Dev. Comp. Immunol.* **2015**, *48*, p. 324-341. https://doi.org/10.1016/j.dci.2014.05.0205.
5. Jaree, P.; Tassanakajon, A.; Somboonwiwat, K. Effect of the anti-lipopolysaccharide factor isoform 3 (ALF*Pm*3) from *Penaeus monodon* on *Vibrio harveyi cells. Dev. Comp. Immunol.* **2012**, *38*, p. 554-560. https://doi.org/10.1016/j.dci.2012.09.001
6. Somboonwiwat, K.; Marcos, M.; Tassanakajon, A.; Klinbunga, S.; Aumelas, A.; Romestand, B.; Gueguen, Y.; Boze, H.; Molin, G.; Bachere, E. Recombinant expression and anti-microbial activity of anti-lipopolysaccharide factor (ALF) from the black tiger shrimp *Penaeus monodon. Dev. Comp. Immunol.* **2005**, *29*, p. 841-851. https://doi.org/10.1016/j.dci.2005.02.004
7. Yang, Y.; Boze, H.; Chemardin, P.; Padilla, A.; Moulin, G.; Tassanakajon, A.; Pugnière, M.; Roquet, F.; Destoumieux-Garzón, D.; Gueguen, Y. NMR structure of rALF-*Pm*3, an anti-lipopolysaccharide factor from shrimp: Model of the possible lipid A-binding site. *Biopolymers* **2009**, *91,* p. 207-220. https://doi.org/10.1002/bip.21119
8. Supungul, P.; Jaree, P.; Somboonwiwat, K.; Junprung, W.; Proespraiwong, P.; Mavichak, R.; Tassanakajon, A. A potential application of shrimp antilipopolysaccharide factor in disease control in aquaculture. *Aquac. Res.* **2017,** *48*, p. 809-821. https://doi.org/10.1111/are.12925
9. Yang, J,; Zhang, Y. I-TASSER server: new development for protein structure and function predictions. *Nucleic Acids Res.* **2015**, *43*, p. W174-W181. https://doi.org/10.1093/nar/gkv342
10. Gordon, J.C.; Myers, J.B.; Folta, T.; Shoja, V.; Heath, L.S.; Onufriev, A. H++: a server for estimating p K as and adding missing hydrogens to macromolecules. *Nucleic Acids Res.* **2005**, *33*, p. W368-W371. https://doi.org/10.1093/nar/gki464
11. Ferguson, A.D.; Wolfram, W.; Eckhard, H.; Buko, L.; Otto, H.; Coulton, J.W.; Kay, D. A. conserved structural motif for lipopolysaccharide recognition by procaryotic and eucaryotic proteins. *Structure* **2000**, *8*, p. 585-592. https://doi.org/10.1016/S0969-2126(00)00143-X
12. Trott, O.; Olson, A.J. AutoDock Vina: improving the speed and accuracy of docking with a new scoring function, efficient optimization, and multithreading. *J. Comput. Chem.* **2010**, *31*, p. 455-461. https://doi.org/10.1002/jcc.21334
13. Kruger, N.J. The Bradford method for protein quantitation. *The protein protocols handbook* **2009**, p. 17-24.
14. Folch, B.; Rooman, M.; Dehouck, Y.. Thermostability of salt bridges versus hydrophobic interactions in proteins probed by statistical potentials. *J Chem Inf Model* **2008**, *48*, p. 119-127. https://doi.org/10.1021/ci700237g
15. Jelesarov, I.; Karshikoff, A. Defining the role of salt bridges in protein stability, *Protein Structure, Stability, and Interactions* **2009**, p. 227-260.
16. Lee, C.W..; Wang, H.J.; Hwang, J.K.; Tseng, C.P. Protein thermal stability enhancement by designing salt bridges: a combined computational and experimental study. *PLoS One* **2014**, 9, p. e112751. https://doi.org/10.1371/journal.pone.0112751